Available online at www.sciencedirect.com
SCIENCE DIRECT
Polymer 46 (2005) 8990–9004
polymer
www.elsevier.com/locate/polymer

Correlations between electrospinnability and physical gelation

Suresh L. Shenoy[a,1,*], W. Douglas Bates[a,2], Gary Wnek[b]

[a]Chemical and Life Sciences Engineering, Virginia Commonwealth University, Richmond, VA 23284-3028, USA
[b]Department of Chemical Engineering, Case Western Reserve University, Cleveland, OH 44106-7217, USA

Received 18 March 2005; accepted 6 June 2005
Available online 10 August 2005

Abstract

Fiber formation by electrospinning is investigated for polymer solutions capable of physical gelation. It is shown that close to the gelation threshold, the combination of thermoreversible junctions and chain entanglements help to stabilize the liquid jet and overcome capillary forces thus giving micro/nano fibers. The effect of cooling time and dissolution temperature besides polymer concentration and molecular weight is clearly demonstrated for polyvinyl alcohol/water and polyvinyl chloride/THF solutions. Finally, the relationship between solvent quality, chain entanglements and poly(vinyl chloride) fiber formation is unequivocally illustrated.

Keywords: Electrospinning; Chain entanglements; Thermoreversible gelation

1. Introduction

In the past decade, electrostatic processing has been routinely employed to obtain ultra-fine fibers [1–3]. The process consists of applying a high voltage to inject charge into a polymer solution of adequate concentration. As the voltage is increased, the drop of liquid presented at the tip of the syringe is attracted to the ground electrode thereby forming a Taylor cone. Above a critical voltage, the electrical energy, a consequence of the injected charge overcomes the surface tension and a continuous jet of liquid is ejected from the Taylor cone and accelerates towards the target electrode. Ultra fine fibers are deposited on the collector due to evaporation of solvent en route. This technique has been employed to numerous polymer/solvent systems to obtain fiber diameters ranging from tens of nanometers to microns. A vast majority of studies reported in the literature concentrate on applications of electrospun fibers [4–9]. However, fundamental understanding of the electrospinning process is limited. Only recently has there been a concerted push to gain deeper insights into the electrospinning process. For example, a number of efforts have concentrated on modeling the whipping instability and fiber diameter [10–17]. However, there has been a lack of knowledge with regards to fiber formation and its relationship to the polymer solution properties. Recently, McKee et al. investigated the solution properties, in particular, the viscosities of linear and branched polyesters, and proposed that fiber formation occurs at the entanglement concentration [18]. Over the past year, we have particularly interested in the effect of polymer solution properties on fiber initiation/formation or 'electrospinnability' (spinnability in electrostatic processing). In this regard we have demonstrated a clear link between chain entanglements in the polymer solution and electrospinnability [19]. In particular, we presented a semi-empirical methodology to a priori predict the transition from electrospraying to electrospinning (or beads to fiber+beads) in good solvents. Additionally, we were also able to predict the transition from fiber+beads to solely fibers (complete fiber formation). The salient features of the approach are described below.

To facilitate predictions from electrospraying (beads) to electrospinning (fibers), as part of our model, we have defined the solution entanglement number $(n_e)_{soln}$, as the ratio of the polymer weight average molecular weight (M_w) to the entanglement molecular weight in solution, $(M_e)_{soln}$.

* Corresponding author. Tel.: +1 216 368 0075; fax: +1 216 368 3016.
E-mail address: suresh.shenoy@case.edu (S.L. Shenoy).
[1] Current address: Department of Chemical Engineering, Case Western Reserve University, Cleveland, OH 44106, USA.
[2] Current address: DuPont AFS Technical, P.O. Box 2 7001, Richmond, VA 23261, USA.

0032-3861/$ - see front matter © 2005 Elsevier Ltd. All rights reserved.
doi:10.1016/j.polymer.2005.06.053

$$(n_e)_{soln} = \frac{M_w}{(M_e)_{soln}} = \frac{\phi M_w}{M_e} \quad (1)$$

Here, M_e is the entanglement molecular weight in the melt and ϕ is the polymer volume fraction. Note that M_e is generally a function of chain topology or geometry and ϕ accounts for the dilution effect due to presence of solvent. Using the results from polymer solution rheology, a correlation was established between fiber initiation (spray to spin transition) and the upturn in zero shear viscosity/M_w plot. Thus in terms of the entanglements, fiber formation is initiated at $(n_e)_{soln} \sim 2$ (or # of entanglements per chain ~ 1). The veracity of this correlation was demonstrated by comparing the predicted polymer concentrations with experimental observations for a number of polymer/solvent systems [19]. The applicability of this approach is clear since a wide range of systems were tested including those involving strong polymer–solvent hydrogen bonding (PEO/water and PVP/ethanol). McKee et al. [18] have reported a similar approach where they employed the entanglement concentration obtained using solution viscosity data, to explain the spray to spin concentration for linear and branched polyesters. With the use of $(n_e)_{soln}$ (or # entanglements per chain), our approach allows a priori prediction of polymer concentration for electrospinnability without having to measure solution viscosities.

Besides fiber initiation, it was demonstrated that the critical concentration for complete fiber formation (no beads or beaded fibers) corresponds to $(n_e)_{soln} = 3.5$ (average of 3–4), i.e. the number of entanglements per chain ~ 2.5 (average of 2–3). Based on the results of Schreiber et al. [20] and Hayahara et al. [21] obtained for conventional dry spinning, we believe this corresponds to the formation of an elastically deformable network under the influence of an elongational flow field. An advantage of our approach is that the only parameter required for the predictions is M_e. Thus, for a given polymer, the spray to spin transition and complete fiber formation (electrospinnability) can be calculated for any concentration/molecular weight space. Note that an underlying assumption of our approach is that chain entanglements are solely responsible for both the upturn in solution viscosity and the formation of the elastic network under the influence of an elongational strain. Therefore, the approach is valid only for the good solvent case where polymer–polymer interactions are negligible.

However, in systems where strong interactions such as hydrogen or ionic bonding are present, polymer–polymer interactions may not be negligible. Increased inter-chain interactions in these systems may serve to stabilize the physical (chain) entanglements by retarding chain disentanglement or forming additional junction points which may facilitate fiber formation at concentrations lower than predicted by Eq. (1). Other factors such as liquid–liquid (L–L) microphase separation [22] in conjunction with vitrification and/or solid–liquid (S–L) phase separation (crystallization) can also serve a similar purpose by creating additional junction points, thereby lowering the concentration threshold for fiber formation. In these systems, the upturn in solution viscosity could be due to the combination of various factors; namely chain entanglements, polymer–polymer interactions and phase separation (L–L, S–L).

In previous work from our laboratory, Kenawy et al. [22] have described a classical system where we believe both L–L and S–L phase separation assists fiber formation. Electrospun mats of ethylene vinyl alcohol copolymers containing 56–71 wt% vinyl alcohol were obtained by electrospinning from rubbing alcohol (70% 2-propanol/30% water, vol:vol). Due to copolymer crystallinity, application of heat (80 °C) was a prerequisite to completely dissolve the copolymer. Upon cooling to room temperature, electrospinning results in EVOH fibers. However, polymer precipitation was always observed, but not until several hours after cooling the solution to room temperature. Since precipitation of EVOH is kinetically quite slow, fiber formation was quite extensive prior to precipitation. Previously, we had speculated that the thermodynamic instability resulting from proximity to liquid–liquid phase separation (upper critical solution temperature or UCST) might be promoting the electrospinning process and subsequent fiber formation [23]. Of course, an additional driving force could be solid/liquid phase separation (crystallization) or a combination of the two (crystallization + UCST). The microscopic crystallites or 'embryonic nucleation sites' comprising of fringed micelles or chain folded crystals can easily serve as junction points where several different polymer chains, come together. The entanglement approach described in our most recent work is clearly not adequate for this type of system. In contrast to the dynamic nature of the physical entanglements, i.e. entanglements formed by crossing over (or knotting), the crystallite junctions are essentially semi-permanent (dissolves at crystallite T_m). Clearly, a combination of the microcrystalline junctions with physical entanglements can facilitate fiber formation.

Additionally, in the course of electrospinning studies, we have frequently observed that some polymer solutions form physical gels quite unlike the precipitation observed for EVOH systems. For example, poly(vinylidene fluoride) (PVDF)/dimethyl formamide (DMF) solutions are prone to form physical gels on cooling to room temperature within a few hours, particularly at high polymer concentrations [24]. The solution can regain its fluidity upon reheating the PVDF/DMF gel. Another system which behaves in a similar manner is completely hydrolyzed ($>99\%$) poly(vinyl alcohol) (PVA)/water [25]. Both systems required application of heat to completely dissolve the semicrystalline polymers (PVDF, PVA). Upon cooling to room temperature, the solutions undergo thermoreversible gelation, quite unlike EVOH (in 2-propanol/water), where precipitation is observed. Interestingly, despite the differences in the final morphology of the solutions (gelation versus precipitation) the mechanisms are quite similar. Therefore, it is possible that mechanisms that promote physical gelation also aid in

extensive fiber formation in these systems (PVDF, PVA). Clearly, the chain entanglement picture is inadequate to explain fiber formation in these systems. In this paper, we attempt to investigate correlations between electrospinnability (fiber formation) and physical or thermoreversible gelation. Since a vast number of synthetic and biopolymers have a tendency to undergo physical gelation, this raises the possibility of obtaining electrospun mats from a number of biopolymers [26,27]. In this paper, however, for the sake of simplicity we concentrate solely on synthetic polymers.

2. Physical gelation of polymer solutions

2.1. Overview

Physical gels are a 3D network of chains in which the junction points are formed as a result of some type of molecular or chain association, e.g. helix formation, complex formation or hydrogen bonding resulting in regions of local order [27,28]. The physical junctions can also arise through phase transitions such as liquid–liquid (L–L) or solid–liquid (S–L) segregation or a combination of the two (L–L + S–L) [27–31]. Consequently, both thermodynamics and kinetics play a vital role in the formation and the morphology of these physical gels. Therefore, these systems can seldom be considered to be in strict thermodynamic equilibrium. Further details on various facets of gel formation, including mechanical and thermal properties and gel morphology are readily available in the literature [26–28].

Briefly, gelation is a function of polymer concentration, molecular weight, temperature, solvent quality and cooling (quench) rate. From an electrospinning perspective, network formation (due to physical junctions) during thermoreversible gelation is of particular interest. For any given solvent this process occurs over a temperature (T) or a concentration (ϕ) range. Thus at a constant T, polymer chains in a dilute solution behave as isolated coils. As the concentration is increased above the overlap concentration (ϕ^*), intermolecular interactions (or embryonic nucleation of microcrystallites) can result in aggregation of several coils forming clusters. Further, an increase in polymer concentration can enhance the size of these clusters as the surrounding free chains are trapped in these aggregates. This is accompanied by a concomitant increase in solution viscosity. Eventually at a critical concentration, a network is formed resulting in physical gelation. This process can be reversed simply by application of heat (or cooling in some cases [26,27]) to eliminate intermolecular interactions (or dissolve microcrystallites) to obtain aggregate-free solutions. Note that based on the mechanism described above, solvent quality can be an important parameter. Thus, choosing low affinity solvents would result in increased polymer–polymer interactions and consequently lead to higher chain aggregation and rapid gelation. For example, polymer/solvent systems which undergo L–L phase separation through spinodal decomposition result in the formation of a network type structure (due to nucleation and growth) when accompanied by vitrification or crystallization [27–31]. However, while low solvent affinity is an important parameter, it is not a necessary condition for physical gelation to occur. Over the past decade, Guenet et al. [26,32,33] have clearly demonstrated that thermoreversible gels can also be obtained in good solvents and hence is not limited to poor solvents as previously believed.

2.2. Spinning and gelation

Our interest in physical gelation was kindled when we realized that an appropriate choice of polymer concentration (ϕ) or temperature (T) would enable us to electrospin polymer solutions before the gelation process commenced. Note that this is different from the traditional gel spinning technique [34], often employed to obtain fibers from PVA, cellulosic esters, acrylonitrile–vinyl chloride copolymers and ultra high molecular weight polyethylene (UHMWPE). Briefly, gel spinning is intermediate between dry and wet spinning and consists of extrusion of a highly concentrated polymer solution or plasticized gel through spinnerets. In electrospinning, the solution concentration is appropriately chosen so that physical gelation occurs on the outer surface of the ejected liquid jet as the solvent evaporates before capillary forces can break up the jet. It is here that the presence of aggregates or clusters in the pregel solutions becomes critical. The parameters (ϕ, T) have to be chosen carefully so that the number of aggregates present in the solution is adequate to stabilize the ejected liquid jet (and aid fiber formation), but not so widespread that physical gelation commences in the syringe. However, obtaining information on the aggregates (number, size) is not a trivial task. Both polymer/solvent thermodynamics and kinetics (slow versus fast cooling, time dependence) play a significant role. Thus, in contrast to jet stabilization by chain entanglements discussed previously [19], a priori prediction of fiber formation in solutions capable of physical gelation is a non-trivial task. Nevertheless, our aim in this paper is at the very least to present a few guidelines (e.g. ϕ, M_w) that can serve as a catalyst for future research in this area. These rules of thumb are empirically deduced by analyzing electrospinning results published in the literature or from experiments performed in our laboratory.

Prior to discussing and analyzing some polymer/solvent systems, we would like to recap some of the results on physical gelation. In general, the threshold concentration above which gelation occurs [$(\phi_{gel})_{threshold}$] > chain overlap concentration (ϕ^*). As ϕ is increased, increased chain overlap eventually leads to chain entanglements ($(n_e)_{soln} - 1$). Thus, usually in a physical gel one can expect two types of junctions to be present; a reversible or semi-permanent junction that can be eliminated by cooling or application of heat as described earlier and a dynamic one, i.e.

entanglement(s). However, note that the presence of chain entanglements is not a necessary condition for physical gelation to occur as has been demonstrated by Boyer et al. [35]. Finally, thermoreversible gelation is not limited to poor solvents and can also occur in good solvents.

In exploring a relationship between fiber formation in electrospinning and physical gelation, we first consider a system where the presence of UCST + S–L phase separation is well known; namely poly(vinyl alcohol) (PVA)/water [25,36,37]. Additionally, the effect of M_w and solvent quality on PVC electrospinning in three different solvents (good, marginal and poor) is explored, namely tetrahydrofuran (THF), morpholine (MOR) and dioxane (DOA).

3. Results and discussion

3.1. PVA/water

Fabrication of electrospun PVA mats has been of particular interest to us due to PVA biocompatibility and its potential use as a tissue-engineering scaffold. PVA is generally produced by saponification or hydrolysis of poly(vinyl esters), generally poly(vinyl acetate). Thus polymer properties (e.g. crystallinity, wettability) are a strong function of the degree of hydrolysis [38]. In addition, tacticity is also an important parameter affecting PVA properties especially crystallinity [38]. Electrospinning of PVA with degree of hydrolysis ranging from 87 to 96% is fairly straightforward [39–41]. However, as reported by Yao et al. [41] from our laboratory, fiber formation in a reproducible manner for fully hydrolyzed PVA (>99%, M_w = 115k) was possible only on addition of a surfactant (Triton X-100). For a 10 wt% PVA in deionized water, the critical surfactant concentration for complete fiber formation was determined to be 0.3% (w/v). It was concluded that the inability to electrospin fully hydrolyzed PVA was probably a combination of high surface tension of water and tendency of PVA to undergo gelation. It was suggested that addition of the surfactant probably retarded PVA gelation while lowering surface tension. More recently, Koski et al. [42] established a correlation between $[\eta]c$ value and electrospinning for PVA/water solutions. Unlike the results obtained in our lab, the authors were able to electrospin high M_w fully hydrolyzed samples. However, the quality of the fibers was poor and included a broad distribution of fibers and beaded fibers. In contrast to these results, Zeng et al. [43] reported complete fiber formation from PVA/water solutions for M_w as high as 195k without use of additives. Thus literature data appears to be inconsistent.

We attempted to investigate reasons for these discrepancies by correlating fiber formation and calculated solution entanglement number, i.e. $(n_e)_{soln}$ (Eq. (1)). If the entanglement analysis were applicable to the PVA/water solution [44–47], one would expect fiber initiation to occur for $(n_e)_{soln} \sim 2$ and complete fiber formation for $(n_e)_{soln} \geq 3.5$ (# entanglements/chain ≥ 2.5) [19]. Table 1 lists calculated $(n_e)_{soln}$ for all the systems considered in this paper. Clearly for PVA/water, there are inconsistencies in the calculated $(n_e)_{soln}$ values which correspond to complete fiber formation. For example, the experimental observations of Koski et al. [42] suggest that the transition from fibers + beads to complete fiber formation occurs for $(n_e)_{soln} \geq 1$ (number of entanglements/chain ≥ 0). On the other hand, Zeng's observations show that the transition value is higher, namely $(n_e)_{soln} \geq 2$ (number of entanglements/chain ≥ 1, i.e. onset of entanglements). Of course, both these values are lower than that predicted by the entanglement analysis [$(n_e)_{soln} \geq 3.5$] for complete fiber formation [19]. We believe the differences in the ability to electrospin high M_w PVA (Yao et al. [41], Koski et al. [42] and Zeng et al. [43]) and lower $(n_e)_{soln}$ values corresponding to fiber formation are related to the propensity of PVA solutions to undergo physical gelation. We attempt to address each issue separately.

3.1.1. Jet stabilization during PVA electrospinning

One of the mechanisms necessary for fiber formation in conventional and electrostatic spinning is the presence of stabilizing junctions such as those provided by chain entanglements. Under the action of an elongational stress, an elastic network is created thereby stabilizing the jet flow against capillary effects. In solutions susceptible to physical gelation, we believe that thermoreversible junctions (responsible for gelation) in conjunction with chain entanglements are responsible for stabilization of the ejected liquid jet from the Taylor cone and consequently fiber formation. From the point of view of obtaining an elastic deformable network (necessary for fiber formation), the thermoreversible junctions (responsible for gelation) are considered to be purely elastic, since in a mechanical test they generally exhibit reversible deformation after a short relaxation. For PVA/water solutions, these thermoreversible junctions are probably 'microcrystallites' formed in solution (S–L phase separation) or a combination of spinodal decomposition (L–L phase separation) together with formation of microcrystallites upon cooling [27,36,37,48]. Each microcrystallite junction is made up of different chains thereby linking different crystallites and forming a network. Prins et al. [36,37] and Komatsu et al. [48] have given more details on the mechanism including the phase diagram to describe PVA gelation. Using the phase diagrams, it appears that PVA fiber formation corresponds to region where sol → gel (see Fig. 5 in Komatsu et al. [48]). For the PVA/water system, the transition from sol to gel is slow (hours) while solutions are generally electrospun immediately after cooling the hot PVA solutions to room temperature. This of course makes it a time dependent process. Therefore, we can expect electrospinning solutions to have some aggregates (due to thermoreversible junctions) but not nearly enough for physical gelation. These aggregates act as additionally stabilizing factors and hence $(n_e)_{soln}$ (Table 1)

Table 1
Compilation of PVA electrospinning results and entanglement number

Reference	$M_w \times 10^3$ (g/mol)	Degree of hydrolysis (%)	Concentration (wt%)	Morphology	$(n_e)_{soln}$ [a]
Koski et al. [42]	9–10	98–99	25	f+b	0.55
	9–10	98–99	35	f	0.8
	13–23	98	21	f+b	0.82
	13–23	98	25	f	1
	13–23	98	27	f	1.1
	13–23	98	31	f	1.3
	31–50	98–99	25	f	2.2
	50–85	97	9	f	1.3
	50–85	97	11	f	1.6
	50–85	97	13	f	1.9
	50–85	97	17	f	2.5
	124–186	>99	6	f+b	1.95
Yao et al. [41]	115	>99	10	f[b]	2.4
Zeng et al. [43]	100	98	6	f+b	1.2
	100	98	8	f+b	1.7
	125	98	6	f+b	1.6
	125	98	8	f	2.1
	195	98	6	f	2.4
	195	98	8	f	3.3
This work	115	>99	6	f+b	1.4
	115	>99	8	f+b	1.9
	115	>99	10	f	2.4

[a] The mean M_w is used whenever molecular weight range is given.
[b] Only upon addition of surfactant.

corresponding to jet stabilization and fiber formation would be lower than previously predicted (3.5, Ref. [19]). Note that in reality, formation of microcrystalline junctions is a complex process and dependent on the stereo-regularity of PVA, degree of hydrolysis and thermal history.

3.1.2. Effect of dissolution temperature

Another issue of importance are the differences in the calculated value of $(n_e)_{soln}$ corresponding to complete fiber formation for high M_w PVA (Table 1). We believe these differences are related to the thermal history of the solutions. It is well known that homogenous PVA solutions are formed at high temperatures (≥ 80 °C) and undergo gelation upon cooling. Additionally, time is an important parameter affecting the number of aggregates (thermoreversible junctions) present in the solution. While both Yao et al. [41] and Koski et al. [42] heated PVA solutions to 80 °C, in the case of Yao et al., the solution was cooled to room temperature prior to electrospinning. On the other hand, Koski et al. electrospun PVA immediately after the PVA had dissolved. No information has been provided about the electrospinning solution temperature. It is entirely possible the cooling time and hence electrospinning temperatures are different in the two cases (Yao et al. and Koski et al.) resulting in differences in the number and size of supramolecular aggregates. The presence of large number of these supramolecular aggregates in the cooled solutions of Yao et al. could result in microgel formation and hence electrospraying of large blobs. In contrast, Zeng et al. [43] heated the PVA solution to 95 °C for a period of >3 h to aid dissolution. No mention has been made of the electrospinning solution temperature. Fibers with diameters ranging from 350 to 700 nm were obtained upon electrospinning an 8 wt% solution of 195k PVA. Zeng's observations suggest that the transition from fiber+beads to fibers is predicted to occur at $(n_e)_{soln} \geq 2$ (Table 1). The reason for the discrepancies between calculated $(n_e)_{soln}$ values corresponding to fiber formation appears to be related to the PVA dissolution temperature. Previous studies on PVA solutions indicate that a temperature of at least 92 °C is needed to completely dissolve PVA [27]. Thus at 80 °C, some micro crystallites (thermoreversible junctions) may be still present. For solutions heated to 95 °C, formation of the supramolecular aggregates upon cooling is slower since crystalline nuclei have been eliminated during the heating process. Consequently, a higher number of chain entanglements would be required [$(n_e)_{soln} \geq 2$] for jet stabilization to compensate for the lower number of aggregates. The same cannot be said for solutions heated to 80 °C.

Another factor not mentioned so far is the effect of M_w. It is well known that in general, the possibility of network formation (and hence gelation) is greater as polymer M_w increases. This is evident from the fact that the gelation temperature increases (or cooling time decreases) as M_w increases. Thus, especially in solutions heated to 80 °C, one would expect to see a strong M_w effect. For the higher M_w polymer (115k), the aggregate formation is much faster and hence by the time the solution is electrospun, gel-like blobs like those reported by Yao et al. are obtained instead of fibers. For the lower M_w polymer, the network formation is

just sufficient to allow fiber formation to occur (but not physical gelation) as has been observed by Koski et al. Heating the high M_w solution to 95 °C eliminates the crystal nuclei thereby slowing down the aggregate formation process and allowing fiber formation on cooling.

To check this hypothesis, we electrospun PVA solutions (same polymer used by Yao et al.; $M_w = 115$k) [41] of different concentrations (6, 8 and 10 wt%) by heating to 95 °C (instead of 80 °C) for about 12 h [49]. Fig. 1(a)–(c) (results tabulated in Table 1) shows optical micrographs of the morphologies obtained upon electrospinning PVA solutions. Note that electrospinning was carried out immediately upon cooling to room temperature. It is clear that complete fiber formation is observed at 10 wt%. The calculated $(n_e)_{soln}$ value corresponding to complete fiber formation also appears to correlate with the onset of entanglements, i.e. $(n_e)_{soln} \geq 2$, in good agreement with values calculated using the experimental observations of Zeng et al. [43]. These findings are in contrast to previously published results [41] discussed in earlier paragraphs when solutions were heated to 80 °C. Furthermore, as PVA concentration is reduced from 10 wt%, beads and beaded fibers are observed, as one would expect. We have also investigated the effect of time. Fig. 1(d)–(f) shows optical micrographs of electrospinning solutions (6–10 wt%) 45 min after the solution has cooled from 95 °C to room temperature. For the 10 wt% solution, as time elapses, development of aggregates (due to formation of thermo-reversible junctions) prevents fiber formation even at 30 kV due to a drastic increase in viscosity. For 8 wt%, gel-like blobs interspersed with a few fibers are obtained. This indicates that for the 8 wt% solution, a sol–gel type

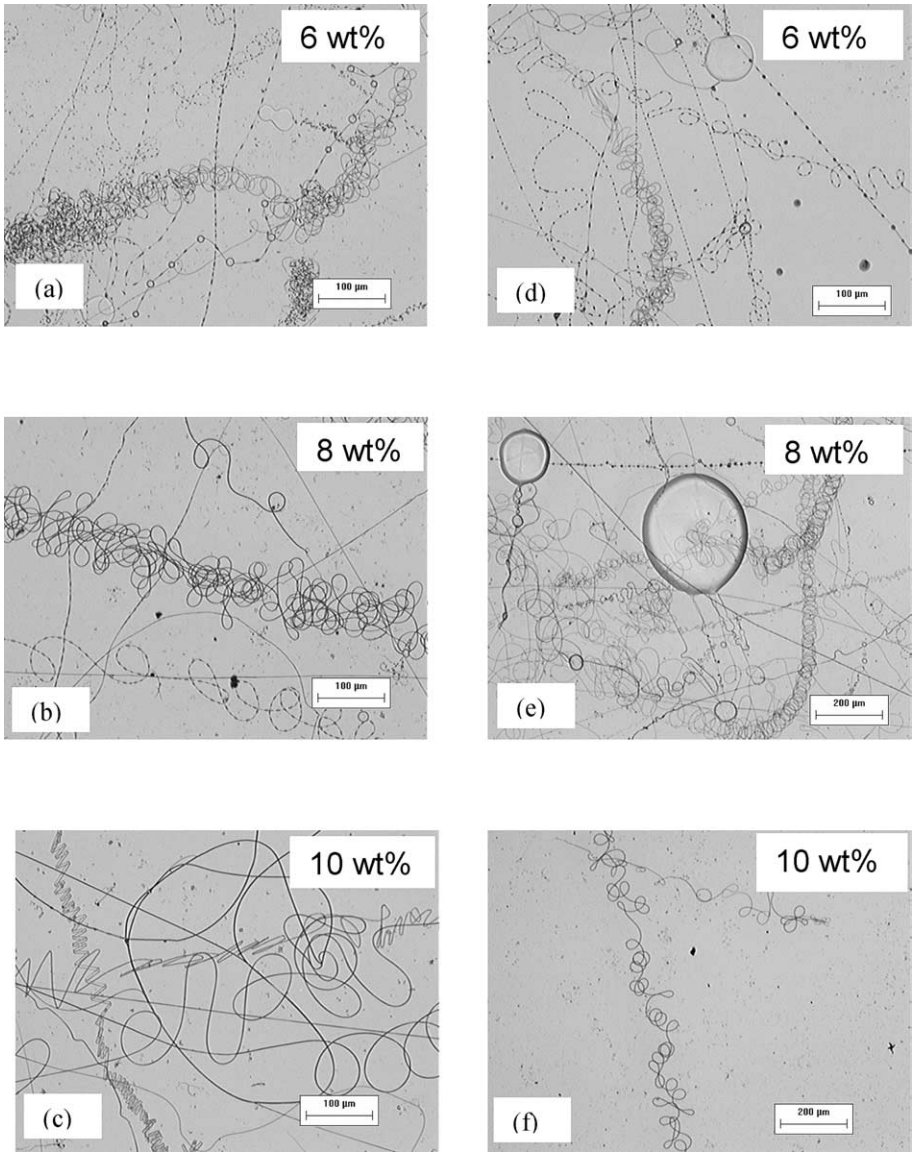

Fig. 1. Optical micrographs of structures obtained by electrospinning PVA/deionized water solutions heated to 95 °C and cooled to room temperature (a) 6 wt% (b) 8 wt% and (c) 10 wt%. The corresponding morphologies 45 min after cooling to room temperature are shown in (d) 6 wt% (e) 8 wt% and (f) 10 wt%.

separation is in progress probably due to continued aggregate formation. This type of separation is limited for the 6 wt% solution (at 45 min) due to lower PVA concentration. Fiber formation is, therefore, a function of time in addition to ϕ and M_w. This time-dependent phenomenon or ageing has been previously discussed in the thermoreversible gelation literature [27]. Thus for PVA solutions, the optimum number of entanglements/chain necessary for fiber formation is a function of M_w, thermal history, time and the temperature of electrospinning. We are currently in the process of evaluating effects of ϕ, M_w and t at various temperatures on fiber formation in solutions capable of gelation and detailed results will be forthcoming in a future publication.

Finally, we conclude this section by considering PVA fiber formation data reported by Koski et al. [42] for the lowest molecular weight (M_w=9–10k). The calculated $(n_e)_{soln}$ values corresponding to fiber formation are <1, i.e. fiber formation occurs in the absence of chain entanglements. We believe a possible explanation for this deviation is higher crystallinity and the effect of functional end groups in lower molecular weight samples. Sato et al. [50] have meticulously investigated the effect of both M_w and chain end groups on physical properties of PVA. The authors concluded that crystallinity increased as M_w decreased irrespective of the chain end functionality. On the other hand, physical properties such as swelling of PVA films in water were observed to be a strong function of end group functionality. It is plausible that both higher crystallinity and interactions between chain end groups can result in stabilization of the jet at significantly lower concentrations than anticipated [$(n_e)_{soln}<1$]. This hypothesis needs to be confirmed by electrospinning at higher temperatures and by using non-interacting functional end groups.

3.2. Poly(vinyl chloride) (PVC)

PVC is a polar polymer where the tacticity has a significant influence on the resulting polymer crystallinity, quite similar to PVA. Lee et al. [51] explored PVC fiber formation by electrospinning as part of a study investigating the effect of mixed solvents. Briefly, Lee et al. concluded that, while pure THF did not facilitate electrospinning of PVC (degree of polymerization=800) due to repeated blockage of the syringe tip, certain solvent ratios of THF/DMF did facilitate fiber formation. In addition, Gupta et al. [52] demonstrated the possibility of side-by-side bicomponent electrospinning using PVC and PVDF.

3.2.1. Dissolution temperature and fiber formation

Our initial interest in PVC was to explore the role of chain entanglements versus the propensity to undergo physical gelation on fiber formation. As a result, we investigated effect of both M_w and solvent quality on PVC fiber formation. Table 2 lists the molecular weight (M_w) of the PVC samples employed for electrospinning. Preliminary experiments indicate that fiber formation (defect free, no beads or beaded fibers) from THF is inconsistent. This problem is particularly acute for the highest M_w sample as shown in Fig. 2(a). However, upon heating the solutions to ~70 °C for a few minutes (and cooling to room temperature), fiber formation from THF is in fact quite extensive (Fig. 2(b)). This observation is analogous to PVA electrospinning described in earlier sections. The key difference is that while PVC/THF solutions are completely miscible (THF is a good solvent), the PVA/water solutions

Table 2
Effect of heating on PVC molecular weight

$M_w\times10^3$ (g/mol)[a]	GPC data obtained in our laboratory		
	Before heating	After heating	96 h after heat treatment
106	108	91	91
233	251	210	208
NA[b]	343	249	260

[a] Values reported by supplier (Aldrich Chemicals).
[b] Not available, value was available from supplier (PolyOne Chemicals).

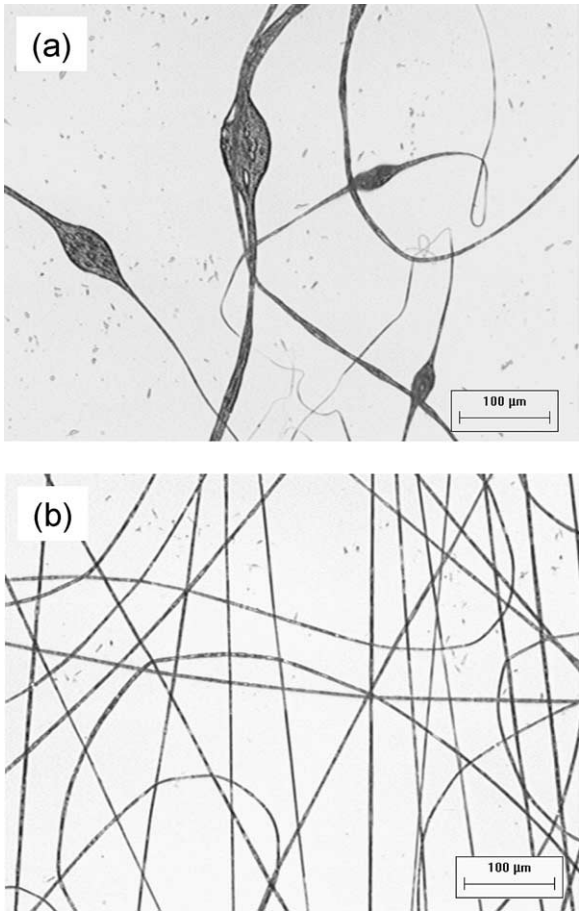

Fig. 2. Effect of heat treatment (70 °C) on the morphology of electrospun fibers from a 9 wt% PVC/THF solution (M_w=249k) (a) before heating and (b) after heat treatment for 10 min.

Table 3
PVC electrospinning results

System	M_w (true)$\times 10^3$ (g/mol)	Observed concentration (wt%)	Predicted concentration (wt%)	Morphology	$(n_e)_{soln}$[a]
PVC/THF	249	6	5.5[b]	f+b	2
	249	9	9.5[c]	f	3.2
	210	7	6.4[b]	f+b	2
	210	11	10.8[c]	f	3.2
	91	10	14.2[b]	f	1.3
	91	16	23.7[c]	f	2.1
PVC/morpholine	249	3.5	8[c]	f	1.3
	249	4.5	8[c]	f	1.7
	210	5	9.4[c]	f	1.7
	91	7	21[c]	f	1.04
PVC/dioxane	210	1	5.8[b]	b	0.3
	210	3	5.8[b]	b	0.9

[a] Calculated using the experimental values, i.e. column 3.
[b] Refers to predicted concentration where fiber formation should be first observed.
[c] Corresponds to predicted concentration where only fibers are expected.

undergo both L–L and S–L phase separation upon cooling. Another interesting observation is the reduction in apparent molecular weight (especially for the highest M_w sample) upon application of heat to PVC/THF solution. This result might explain the difficulty in electrospinning PVC solutions (especially high M_w) prior to heating. Gel permeation chromatography results given in Table 3 shows that for the highest molecular weight sample, M_w decreases from 343k to 249k after heat treatment. Interestingly, M_w appears to increase again to 260k 96 h after heat treatment and cooling. At present, we are not sure if this is simply within the limits of error of the instrument or if it is a genuine trend since we have not investigated M_w as a function of time for $t>96$ h. Nevertheless, based on published reports [26,27,53,54], we believe aggregation of syndiotactic sequences in PVC is responsible for the apparent higher M_w prior to heating. The aggregation is extensive enough to prevent consistent defect-free fiber formation. Application of heat destroys the aggregates and promotes fiber formation [27]. This hypothesis is also validated by published light scattering and NMR spectroscopy data on pregel PVC solutions [26,27]. We believe this phenomenon is restricted to the high M_w sample since the reaction methodology employed to obtain high M_w PVC (traditionally low reaction temperature) also results in an increase in number of the syndiotactic sequences consequently increasing aggregation [27]. While the change in M_w on heating is negligible for the 90k and 210k samples, the issue of inconsistent fiber formation (in the absence of heating) nevertheless remains true. It is possible that for these samples aggregation is very subtle at the solutions concentrations employed for GPC measurements (0.6 wt%). On the other hand significantly higher concentrations are required for PVC fiber formation (by electrospinning 10–16 wt% depending on the M_w). At these concentrations, considerable levels of aggregation may be present resulting in inconsistent fiber formation.

For the sake of consistency in all calculations we have employed the M_w obtained in our laboratory by GPC after heating the solutions. Using $(M_e)_{PVC}=4310$ g/gmol [44–46,55] in the entanglement analysis, i.e. Eq. (1), it is predicted that for the 210k sample, fiber initiation (mixture of beads+fibers) should commence around 6.4 wt% ($(n_e)_{soln}=2$) and only fibers should be obtained for concentrations ≥ 10.8 wt% ($(n_e)_{soln}=3.5$). Fig. 3 shows the optical micrographs of the morphologies obtained by electrospinning PVC solutions of different concentrations from THF. Fiber initiation occurs $\sim$7 wt% and for 11 wt% only fibers are obtained thus validating our predictions. For solutions with higher PVC concentration (12 wt%), high solution viscosity inhibits extensive fiber formation. Eventually 14 wt% PVC solutions undergo a partial sol to gel transition in approximately 72 h. On the other hand, for the 11 wt% solution no gelation was observed even after a week. The observation of PVC gelation in THF came as a surprise to us. While there appears to be a wealth of information on PVC gelation in a variety of solvents [26,27], gel formation in THF, a good solvent, has not been reported, though it is a distinct possibility given the results of Guenet et al. [32,33]. What is unclear and not the subject of our study is the PVC gelation mechanism in good solvents such as THF (as opposed to poor solvents), i.e. microcrystallites or polymer–solvent complexes. Irrespective of the gelation mechanism, our interest lies in determining correlations between PVC gelation in good solvents such as THF and fiber formation.

3.3. Effect of PVC M_w on mechanism of jet stabilization

In this section, we investigate the effect of PVC M_w on jet stabilization mechanisms during electrospinning [56]. Table 3 presents the results for $M_w=343$k, 251k and

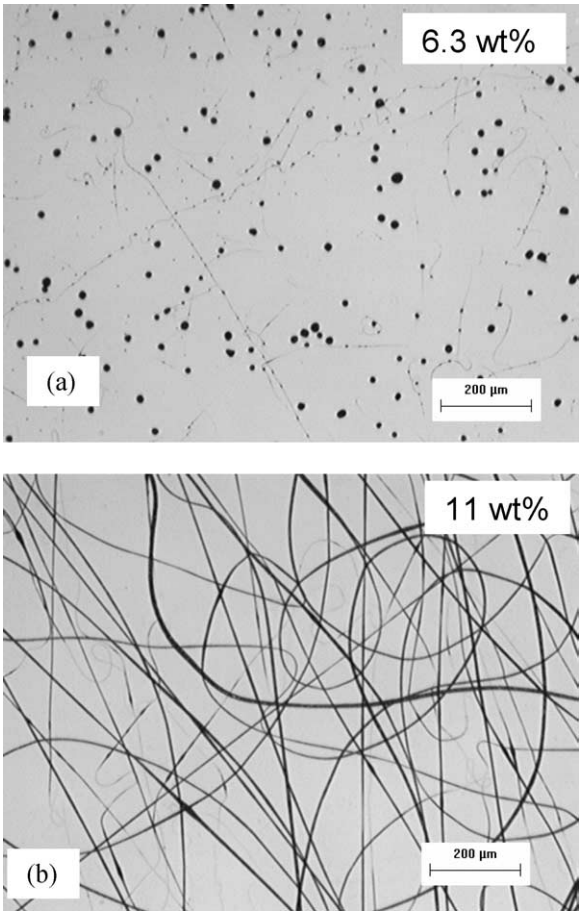

Fig. 3. Electrospinning of PVC (M_w=210k)/THF solutions: (a) 6.3 wt% and (b) 11 wt%.

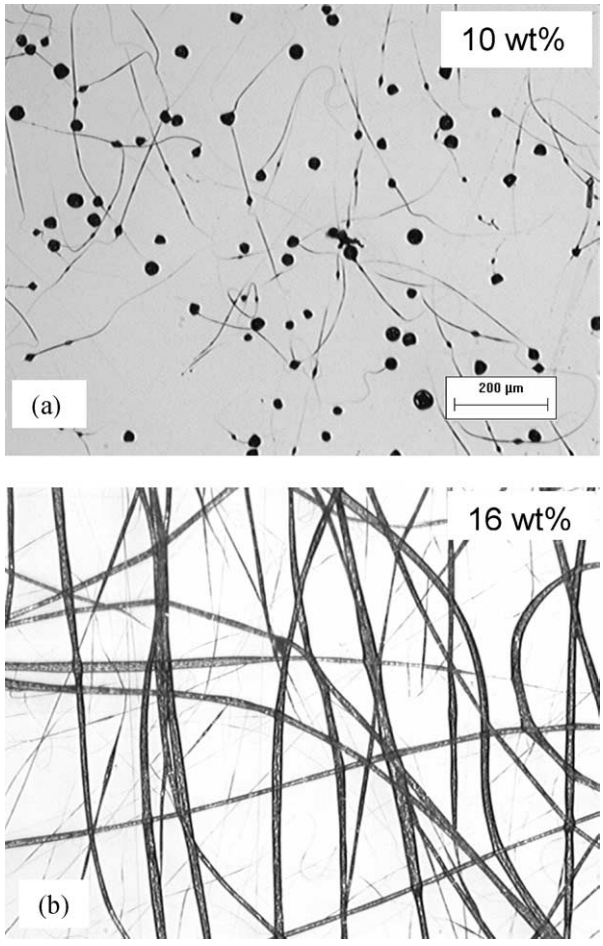

Fig. 4. Electrospinning of PVC (M_w=91k)/THF solutions: (a) 10 wt% and (b) 16 wt%.

108k. The true M_w for these samples obtained by GPC correspond to 249k, 210k and 91k, respectively. Note that the true M_ws are used in Eq. (1) to calculate $(n_e)_{soln}$ corresponding to fiber formation. For the higher M_w sample, i.e. 249k, the entanglement analysis predicts that the transition from beads to fibers+beads occurs ~5.5 wt% ($(n_e)_{soln}$=2) and only fibers should be obtained for concentrations ≥9.5 wt% ($(n_e)_{soln}$≥3.5). The experimental results reported in Table 3 for the 249k PVC are in good agreement with the predictions. Thus for 249k and 210k PVC, chain entanglements are responsible for jet stabilization and fiber formation. For the lower M_w solutions (91k), the corresponding transitions are predicted to be ~14.2 and 23.7 wt%. Surprisingly, as shown in Fig. 4, fiber initiation occurs ~10 wt% and complete fiber formation (no beads or beaded fibers) is observed around 16 wt%. Reconciling the experimental observations with the entanglement analysis (Eq. (1)) for the lower molecular weight (91k) PVC is difficult. Based on arguments made for PVA/water solutions, it is plausible that for the 91k sample chain entanglements may not be the sole mechanism for formation of elastic network and hence fiber formation. This hypothesis is validated by the fact that for an 18 wt% solution, gelation occurs within 3–4 h. Interestingly, the calculated $(n_e)_{soln}$ values corresponding to complete fiber formation (M_w=91k) is ~2, signifying the presence of one entanglement/chain. Thus supramolecular aggregates (due to thermoreversible junctions) in the lower M_w PVC solutions play a vital role in fiber formation.

However, an obvious question remains unanswered. Upon decreasing M_w from 249k, at what point does the mechanism for fiber formation change from simply physical entanglements to a combination of entanglements and thermoreversible junctions (corresponding to gelation)? We believe the answer lies in probing the M_w dependence of $(\phi_{gel})_{threshold}$ and $(\phi_{el})_{fiber}$, where $(\phi_{gel})_{threshold}$ is the threshold concentration (volume fraction) at which gelation occurs and $(\phi_{el})_{fiber}$ is the concentration (volume fraction) at which an elastic network is obtained giving only fibers. Decreasing M_w increases both the $(\phi_{gel})_{threshold}$ and $(\phi_{el})_{fiber}$. From a theoretical perspective, previous studies on atactic polystyrene (aPS) gelation in poor solvents have suggested that [28,35]

$$(\phi_{gel})_{threshold} \propto (M_w)^{-0.5} \quad (2)$$

On the other hand, for PVC/THF solutions, Eq. (1) can be

rewritten as

$$(\phi_{el})_{fiber} = \frac{3.5M_e}{M_w} = \frac{15,085}{M_w} \quad (3)$$

which implies that $(\phi_{el})_{fiber} \propto (M_w)^{-1}$. Thus, the M_w dependence of $(\phi_{gel})_{threshold}$ is weaker.

In Fig. 5, we plot and compare both the theoretical and experimental dependence of $(\phi_{gel})_{threshold}$ and $(\phi_{el})_{fiber}$ on M_w. The experimental values of $(\phi_{gel})_{threshold}$ for all samples was assumed to the polymer volume fraction in solution which results in gelation in approximately 6 h. Though this time frame is completely arbitrary, it still allows us to show that the transition from a purely entanglement mechanism to combination of entanglement and gelation is due to the weak M_w dependence of $(\phi_{gel})_{threshold}$. Obtaining the experimental $(\phi_{el})_{fiber}$ is fairly straightforward and consists of determining the concentration corresponding to complete fiber formation by electrospinning different M_w PVC/THF solutions.

To obtain theoretical $(\phi_{gel})_{threshold}$, we have employed experimentally determined value for the 91k sample as the reference, i.e. $(\phi_{gel})_{threshold\ 91} = 0.125$ vol% (0.18 wt fraction). Then, theoretical $(\phi_{gel})_{threshold}$ for any molecular weight samples is calculated using Eq. (4).

$$(\phi_{gel})_{threshold\ M_w} = (\phi_{gel})_{threshold\ 91}\left(\frac{M_{w91}}{M_w}\right)^{0.5} \quad (4)$$

Note that Eq. (4) is directly obtained from Eq. (2). For the current samples, M_w will be 210k and 249k, respectively. For $(\phi_{el})_{fiber}$, the theoretical curve is obtained using Eq. (3). Note that this curve is valid for PVC/THF solutions only since it involves $(M_e)_{PVC}$.

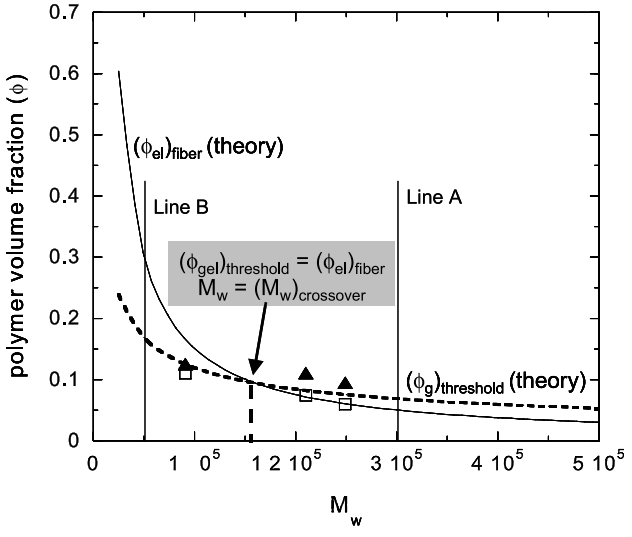

Fig. 5. Determination of the critical M_w for PVC/THF solutions where fiber formation mechanism changes from simply physical entanglements to a combination of entanglements and thermoreversible gelation. The dashed line corresponds to $(\phi_g)_{threshold}$ calculated using Eq. (4) while the bold line is $(\phi_{el})_{fiber}$ calculated using Eq. (3).The experimental values of $(\phi_g)_{threshold}$ (▲) and $(\phi_{el})_{fiber}$ (□) have been plotted for comparison.

Fig. 5 clearly shows that for $(\phi_{el})_{fiber}$ there is excellent agreement between theory and experiment for the higher M_ws (210k and 249k). However, for the lower M_w the experimental value is considerably lower than predictions (0.11 versus 0.176). For $(\phi_{gel})_{threshold}$, the experimental value appears to be higher than the theoretical predictions (0.11 versus 0.082 for 210k and 0.095 versus 0.076 for 249k). Clearly the experimental M_w dependence of $(\phi_{gel})_{threshold}$ is weaker than predicted by Eq. (2). This maybe ascribed to the differences in the gelation mechanism. Note that Eq. (2) was deduced theoretically for aPS. Gelation of aPS has been attributed to a combination of L–L phase separation and vitrification [29,30,35]. In contrast, PVC/THF gelation is either a result of S–L phase separation (microcrystallites) or polymer–solvent complexes [26,27,32,57]. Thus strictly speaking Eq. (2) is not valid for PVC/THF. In fact, we expect $(\phi_{gel})_{threshold}$ to be weaker function of M_w (than Eq. (2)) since the effect of chain length on polymer crystallization or polymer/solvent complexation is insignificant for the lengths under consideration (91k to 249k). Our experimental observations for $(\phi_{gel})_{threshold}$ (Fig. 5) clearly validate this hypothesis.

In Fig. 5, we clearly notice a crossover of the $(\phi_{gel})_{threshold}$ and $(\phi_{el})_{fiber}$ curves at $(M_w)_{crossover} \sim 155$k. For PVC samples with $(M_w)_{crossover} > 155$k, as one increases the PVC concentration (depicted as line A in Fig. 5), its is clear that $(\phi_{el})_{fiber}$ is attained prior to $(\phi_{gel})_{threshold}$. Thus we can conclude that for the 249k and the 210k solutions, fiber formation at ~9 wt% ($\phi = 0.06$) and 11 wt% ($\phi = 0.074$), respectively, is primarily due to stabilization by chain entanglements. In contrast for $M_w < (M_w)_{crossover}$, upon increasing PVC concentration (line B in Fig. 5), one encounters $(\phi_{gel})_{threshold}$ prior to $(\phi_{el})_{fiber}$. Therefore, for the 91k sample, thermoreversible junctions in conjunction with chain entanglements (since $(n_e)_{soln} \geq 2$ or number of entanglements ≥ 1) are responsible for jet stabilization.

3.4. Effect of solvent quality on PVC electrospinning

From the discussion so far, it is clear that fiber formation in electrospinning is strongly influenced by the propensity of the polymer solution to gel. This implies that solvent quality significantly affects gelation and consequently fiber formation during electrospinning. For example, it has been suggested that crystallinity in PVC gels is a function of the polymer–solvent interactions [26,27]. Similar results have been reported for PVA gels [58]. More recently Hong et al. [59] have extensively investigated the effect of solvent quality on the PVC ($M_w = 500$k) gelation behavior. Three solvents having similar molar volumes and functional groups but dissimilar charge density arrangements and hence dipole moments; namely tetrahydrofuran (THF), morpholine (MOR) and dioxane (DOA) were employed. The results relevant to our work are briefly summarized:

(i) The strength of the polymer–solvent interactions

was established to be PVC/THF > PVC/MOR > PVC/DOA. In addition, by extrapolating the second virial coefficient to zero, i.e. $A_2 = 0$, the θ-temperatures for PVC/THF, PVC/MOR and PVC/DOA were determined to be approximately 0, 56 and 70 °C, respectively.

(ii) Formation of aggregates in the solution was demonstrated to be a function of solvent quality; i.e. DOA > MOR. Light scattering did not reveal any significant aggregation in THF solutions.

(iii) Not surprisingly the ease of gelation was determined to be a function of solvent quality, namely; DOA > MOR. The gelation concentration threshold was measured to be about 2.2 wt% in DOA and about 4 wt% in MOR. No gelation was observed in PVC/THF solutions at 6 wt%.

(iv) The gelation mechanism in MOR and DOA was speculated to be the result of both L–L and S–L phase separations.

From our perspective, this in-depth investigation by Hong et al. [59] offers a unique opportunity to investigate the effect of solvent quality on PVC electrospinning. Note that despite the lower molecular weights used in our study, we expect the trends described above (i)–(iv) to be valid for our samples.

PVC/MOR ($M_w = 249$k, 210k, 91k) and PVC/DOA ($M_w = 210$k) solutions were electrospun at various concentrations. The details of the experiments are given in Ref. [56]. While the experimental observations for 210k are described below, the remaining results are tabulated in Table 3. During the course of our experiments, we observed that the 7 wt% PVC/MOR and 4 wt% PVC/DOA solutions undergo rapid gelation upon cooling. Lowering polymer concentration could allow us enough time to attempt electrospinning by retarding onset of gelation. Accordingly, Figs. 6 and 7 show optical micrographs of the morphologies obtained by electrospinning PVC/MOR solutions with concentrations ranging from 4 to 6 wt%. For the 4 wt% PVC/MOR solution (Fig. 6), electrospinning upon cooling clearly yields fiber with some beads (Fig. 6(a)). In addition, large blobs are also observed indicating presence of pregel aggregates or clusters in the solution. In contrast, electrospinning of the same solution 48 h after cooling to room temperature, yields large blobs/particles and no fibers as shown in Fig. 6(b). Additionally, formation of a steady jet is not observed. The syringe tip appears to spit gigantic gel-like blobs towards the target upon application of the voltage. This time dependent behavior is clearly a sign of onset of sol to gel transition. Fig. 7 shows the morphology obtained by electrospinning 5 and 6 wt% PVC/MOR solutions immediately upon cooling. The micrographs in Fig. 7(a) and (b) clearly demonstrate that for these concentrations, an elastic deformable network is formed thereby supporting fiber formation. After 24 h, microgel formation is evident for the 5 wt% solution based on the presence of blobs in Fig. 7(c),

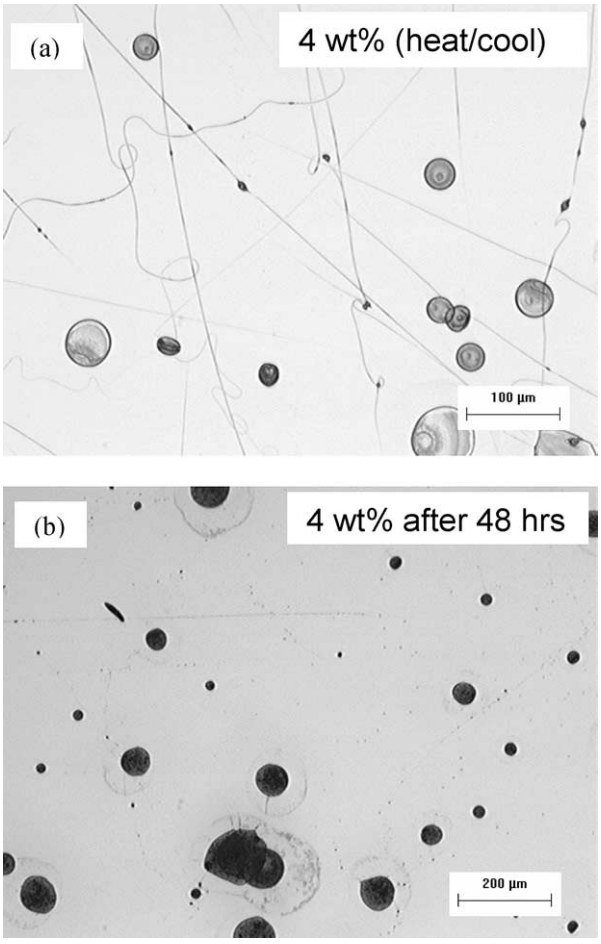

Fig. 6. Effect of time on electrospinning 4 wt% PVC ($M_w = 210$k)/morpholine solutions: (a) Immediately on cooling and (b) 48 h after cooling to room temperature.

while the 6 wt% solution completely undergoes gelation (Fig. 7(d)) and cannot be electrospun.

For the PVC/DOA solutions, the PVC concentrations had to be reduced to avoid rapid gelation upon cooling, in good agreement with the results of Hong et al. (conclusion (ii) in Section 3.4). Fig. 8 shows the optical micrographs of 1 and 3 wt% PVC/DOA solutions electrospun at conditions identical to PVC/THF and PVC/MOR. At 1 wt%, only beads are observed. On the other hand, spindle shaped beads are observed at 3 wt%. Electrospinning of the 4 wt% solution was not possible since it underwent rapid gelation on cooling to room temperature. Clearly while we are close to the transition for fiber initiation, the rapidity of physical gelation limits our ability to electrospin PVC/DOA solutions at concentrations where fiber formation maybe a possibility.

The higher and lower M_w PVC (249k and 91k) was also employed to check effect on PVC fiber formation in MOR. The results are listed in Table 3. As expected, concentration corresponding to complete fiber formation increases as M_w; namely, 7 wt% for 91k instead of 5 wt% for 210k. At concentrations > 9 wt% for the 91k PVC (versus 7 wt% for

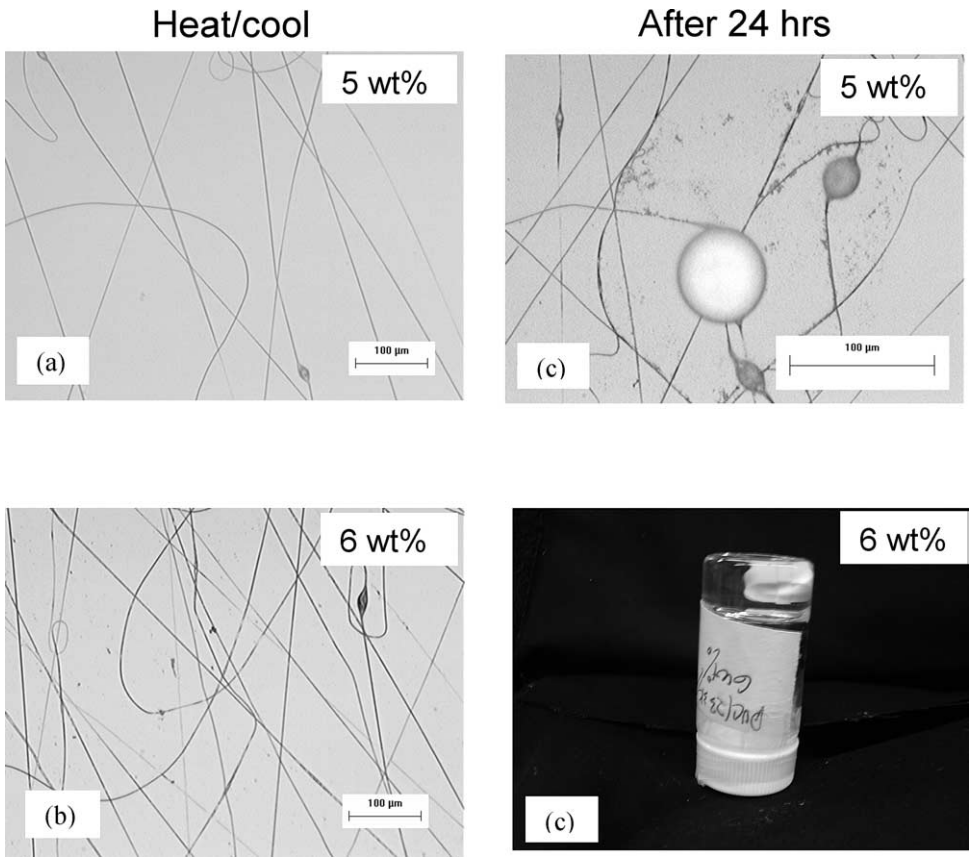

Fig. 7. Electrospinning 5 ((a) and (c)) and 6 ((b) and (d)) wt% PVC (M_w = 210k)/morpholine solutions as a function of time: (a) 5 wt% immediately on cooling, (b) 6 wt% immediately on cooling (c) 5 wt% solution 24 h after cooling to room temperature (d) physical gelation of 6 wt% solution.

210k), the solution undergoes gelation rapidly resulting in an unstable liquid jet. For the higher M_w solution, i.e. 249k, fiber formation is observed at 4 wt%, while gelation occurs rapidly at higher PVC concentrations.

In summary, the critical concentration above which only fibers are obtained is a function of both, solvent quality (THF > MOR > DOA) and M_w. For PVC/MOR the critical concentrations are lower than in THF, namely 4 versus 9 wt% for the 249k sample, 5 versus 11 wt% for the 210k sample and 7 versus 16 wt% for the 91k sample. On the other hand, PVC fiber formation from dioxane (DOA) solutions was not possible due to the tendency to undergo rapid gelation. These results are in very good agreement with the solvent quality trend determined by Hong et al.; namely (THF > MOR > DOA) [59]. For the 249k and the 210k sample in THF, we believe that formation of elastic network is probably a result of chain entanglements since $(n_e)_{soln} \sim 3.5$, while for the 91k sample fiber formation is due to a combination of chain entanglements and aggregate formation since $(n_e)_{soln} \geq 2$). In MOR (both 210k and 91k), it appears that fiber formation is also due to a combination of pregel aggregates and chain entanglements. One can directly correlate this to the tendency for physical gelation due to L–L and S–L phase behavior. However, in MOR, fiber formation is obtained for $(n_e)_{soln} \geq 1$. These results are in contrast to the calculated $(n_e)_{soln}$ values (≥ 2) obtained for PVC/THF solutions corresponding to complete fiber formation. We believe that this due to the lower solvent quality of MOR than THF. Interestingly, these results also suggest that in THF the contribution from chain entanglement and thermoreversible junctions maybe almost equal. However, in MOR (a marginal solvent), almost all the stabilization is primarily due to the presence of thermoreversible junctions ($(n_e)_{soln} \geq 1$ or number of chain entanglements ≥ 0 or minimal). For the 3 wt% PVC/DOA (91k) solution, $(n_e)_{soln} < 1$, indicating we are below the entanglement regime and thus it is no surprise that fiber formation is inhibited.

4. Final thoughts

It is clear from our results (similar to conventional fiber spinning [34]) that there is no single mechanism describing fiber formation in electrospinning. The single most important parameter is stabilization of the ejected liquid jet against capillary effects long enough for solidification to occur principally through solvent evaporation. For wet electrospinning, the solidification will be a result of the coagulation of the outer layer of the liquid jet (similar to wet

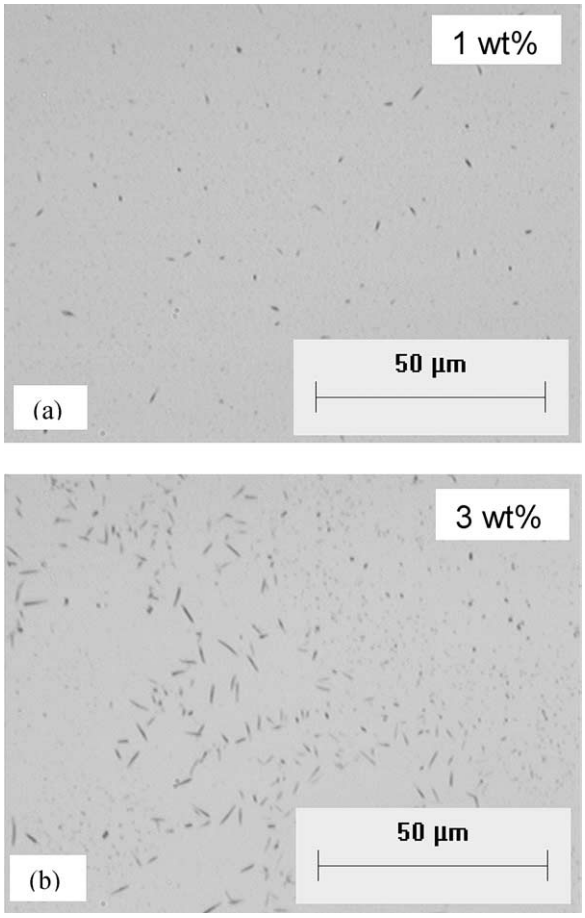

Fig. 8. Electrospinning of PVC/dioxane (M_w=210k) solutions (a) 1 wt% and (b) 3 wt% immediately upon cooling.

spinning). In the previous paper we looked at systems in dry electrospinning (similar to conventional dry spinning) where chain entanglements were the sole reason for jet stabilization. This mechanism appears to be limited to the good solvent case and where polymer–polymer interactions are negligible. In this paper, we have identified yet another probable mechanism of jet stabilization. In polymers which can undergo gelation even in good solvents, thermoreversible junctions in combination with chain entanglements provide stabilization long enough for jet solidification and hence fiber formation. However, in good solvents, as seen from the M_w study (PVC/THF), this double mechanism may be restricted to lower M_w polymers. This is primarily because of the unequal dependence of $(\phi_{el})_{fiber}$ and $(\phi_{gel})_{threshold}$ with M_w (Eqs. (1)–(3)).

As shown in Fig. 5, both $(\phi_{el})_{fiber}$ and $(\phi_{gel})_{threshold}$ increase with reduction of M_w. The intersection of the two curves ($(\phi_{el})_{fiber}$, $(\phi_{gel})_{threshold}$ versus M_w) gives the critical M_w, below which gelation becomes important. Therefore, below this M_w, both chain entanglements and thermoreversible junctions contribute to jet stabilization ($(n_e)_{soln} \geq 2$). In contrast above this critical M_w, only chain entanglements are important and fiber formation can be predicted a priori using Eq. (1). For PVC, this critical value is ~155k. Note that this is an approximate value since we have previously established that Eq. (4) overestimates $(\phi_{gel})_{threshold}$ (due to differences in gelation mechanism). Similar plots can be constructed for other polymer/solvent systems using the corresponding M_e values and determining the gelation threshold (Eq. (4)).

Finally, solvent quality is another important parameter that has been investigated in this paper. Our analysis shows that as solvent quality decreases, the jet stabilization predominantly occurs due to presence of thermoreversible junctions. Such is the case for PVC/MOR where the calculated value of $(n_e)_{soln}$ corresponding to fiber formation is ≥ 1. Therefore, while physical entanglements may be present (# entanglements per chain ≥ 0), they are secondary to the thermoreversible junctions. An advantage of using a marginal solvent (such as MOR for PVC) is that the polymer concentration corresponding to fiber formation is considerably less than for a good solvent. Finally, for a poor solvent like DOA, physical gelation is extremely rapid. Hence for concentrations where physical entanglements occur, gelation is too rapid for electrospinning to be attempted. At lower concentrations, electrospinning yields spindle shaped beads. This may be due to lack of any chain entanglements; $(n_e)_{soln} < 1$. A logical conclusion is that presence of chain entanglements even as a secondary means of jet stabilization may be necessary for fiber formation.

As a final point, note that all our electrospinning experiments were performed at room temperature. Since gelation (aggregation) is affected by temperature, it is logical to expect that electrospinning at higher temperatures might offer unique opportunities for systems, which undergo gelation at room temperature (e.g. PVC/MOR, PVC/DOA).

5. Conclusions

In this paper, we have shown that fiber formation by electrospinning for solutions capable of physical gelation is possible. The conclusions of the investigation are summarized below:

(a) Fiber formation from PVA/water solutions is clearly a function of the dissolution temperature. Defect free fibers from high fully hydrolyzed M_w PVA are obtained only when the dissolution temperatures is high enough (>92 °C) to ensure elimination of embryonic crystallites.
(b) The contribution from chain entanglements, i.e. $(n_e)_{soln}$ is a function of the dissolution temperatures. For lower temperatures, i.e. 80 °C, fiber formations corresponds to $(n_e)_{soln} \geq 1$ indicating the absence of chain entanglements. The thermoreversible junctions are solely responsible for stabilizing the liquid jet. In contrast for dissolution temperatures ≥ 92 °C, fiber formation corresponds to $(n_e)_{soln} \geq 2$. Thus, the liquid jet is

stabilized by a combination of chain entanglements and thermoreversible junctions.

(c) In addition to the dissolution temperatures, the elapsed time is another important factor, which influences fiber morphology.

(d) The fiber formation mechanism for PVC in a good solvent (THF) is a balance between the M_w dependence of the gelation concentration, i.e. $(\phi_{gel})_{threshold}$ and the concentration corresponding to fiber formation due to chain entanglements only, i.e. $(\phi_{el})_{fiber}$. For higher M_w (249k and 210k) PVC, $(\phi_{el})_{fiber}$ or chain entanglements dominate while at the lower M_w (91k) the liquid jet is stabilized by both, chain entanglements and thermoreversible junctions.

(e) Besides M_w, solvent quality plays a vital role in determining the chain entanglement contribution. For marginal solvents such as morpholine, at low concentrations where chain entanglements are below the critical value ($(n_e)_{soln} \geq 3.5$), significant number of thermoreversible junctions help to stabilize the jet and form fibers. Thus for PVC/MOR fiber formation is observed for $(n_e)_{soln} \geq 1$. Time is an important parameter for such systems. Longer cooling times results in abundance of the thermoreversible junctions, which increases viscosity dramatically preventing fiber formation.

(f) On the other hand, if the solvent quality is poor as observed for PVC/dioxane, gelation is rapid due to increased polymer aggregation and hence fiber formation is not observed.

(g) For solutions capable of physical gelation, fiber formation is thus a function of polymer concentration, M_w, temperature, solvent quality and cooling time.

Acknowledgements

The authors would like to thank PolyOne for kindly donating sample of Geon 407. In addition the authors wish to thank Mr Umit Makal at VCU, Chemical Engineering for GPC measurements. The authors would also like to thank DARPA (Bio-Optic Synthetic Systems Program) and the NASA Office of Space Sciences for generous support.

References

[1] Li D, Xia YN. Adv Mater 2004;16:1151–70.
[2] Huang ZM, Zhang YZ, Kotaki M, Ramakrishna S. Compos Sci Technol 2003;63:2223–53.
[3] Frenot A, Chronakis IS. Curr Opin Colloid Interface Sci 2003;8:64–75.
[4] Kenawy ER, Bowlin GL, Mansfield K, Layman J, Simpson DG, Sanders EH, et al. J Controlled Release 2002;81:57–64.
[5] Matthews JA, Boland ED, Wnek GE, Simpson DG, Bowlin GL. J Bioact Compat Polym 2003;18:125–34.
[6] Li WJ, Laurencin CT, Caterson EJ, Tuan RS, Ko FK. J Biomed Mater Res 2002;60:613–21.
[7] Schreuder-Gibson H, Gibson P, Senecal K, Sennett M, Walker J, Yeomans W, et al. J Adv Mater 2002;34:44–55.
[8] Wang XY, Drew C, Lee SH, Senecal KJ, Kumar J, Samuelson LA. J Macromol Sci, Pure Appl Chem 2002;A39:1251–8.
[9] Zussman E, Yarin AL, Weihs D. Exp Fluids 2002;33:315–20.
[10] Yarin AL, Koombhongse S, Reneker DH. J Appl Phys 2001;89:3018–26.
[11] Yarin AL, Koombhongse S, Reneker DH. J Appl Phys 2001;90:4836–46.
[12] Shin YM, Hohman MM, Brenner MP, Rutledge GC. Appl Phys Lett 2001;78:1149–51.
[13] Shin YM, Hohman MM, Brenner MP, Rutledge GC. Polymer 2001;42:9955–67.
[14] Spivak AF, Dzenis YA, Reneker DH. Mech Res Commun 2000;27:37–42.
[15] Fridrikh SV, Yu JH, Brenner MP, Rutledge GC. Phys Rev Lett 2003;90.
[16] Feng JJ. J Non-Newtonian Fluid Mech 2003;116:55–70.
[17] Feng JJ. Phys Fluids 2002;14:3912–26.
[18] McKee MG, Wilkes GL, Colby RH, Long TE. Macromolecules 2004;37:1760–7.
[19] Shenoy SL, Bates WD, Frisch HL, Wnek GE. Polymer 2005;46:3372–84.
[20] Schreiber HP, Rudin A, Bagley EB. J Appl Polym Sci 1965;9:887–92.
[21] Hayahara T, Takao S. J Appl Polym Sci 1967;11:735–46.
[22] Kenawy ER, Layman JM, Watkins JR, Bowlin GL, Matthews JA, Simpson DG, et al. Biomaterials 2003;24:907–13.
[23] Young TH, Cheng LP, Hsieh CC, Chen LW. Macromolecules 1998;31:1229–35.
[24] Bates WD, Barnes CP, Ounaies Z, Wnek GE. Polym Prepr 2003;44:114.
[25] Kawanishi K, Komatsu M, Inoue T. Polymer 1987;28:980–4.
[26] Guenet JM. Thermoreversible gelation of polymers and biopolymers. San Diego: Academic Press; 1992.
[27] te Nijenhuis K, editor. Thermoreversible networks: Viscoelastic properties and structure of gels.
[28] Keller A. Faraday Discuss 1995;1–49.
[29] Tan HM, Chang BH, Baer E, Hiltner A. Eur Polym J 1983;19:1021–5.
[30] Tan H, Moet A, Hiltner A, Baer E. Macromolecules 1983;16:28–34.
[31] Wellinghoff S, Shaw J, Baer E. Macromolecules 1979;12:932–9.
[32] Guenet J-M. Trends Polym Sci (Cambridge, UK) 1996;4:6–11.
[33] Guenet JM. Macromol Symp 1997;114:97–108.
[34] Ziabicki A. Physical fundamentals of fiber formation 1976.
[35] Boyer RF, Baer E, Hiltner A. Macromolecules 1985;18:427–34.
[36] Pines E, Prins W. Macromolecules 1973;6:888.
[37] Feke GT, Prins W. Macromolecules 1974;7:527–30.
[38] Pritchard JG. Poly(vinyl alcohol) basic properties and uses. London: Gordon and Breach, Science Publishers Ltd; 1970.
[39] Scuador Jr AE, Shaw MT, Mather PT. Mater Res Soc Symp Proc 2001;661:KK5 9/1–KK5 9/6.
[40] Ding B, Kim H-Y, Lee S-C, Shao C-L, Lee D-R, Park S-J, et al. J Polym Sci, Part B: Polym Phys 2002;40:1261–8.
[41] Yao L, Haas TW, Guiseppi-Elie A, Bowlin GL, Simpson DG, Wnek GE. Chem Mater 2003;15:1860–4.
[42] Koski A, Yim K, Shivkumar S. Mater Lett 2004;58:493–7.
[43] Zeng J, Hou H, Wendorff JH, Greiner A. Polym Prepr (Am Chem Soc, Div Polym Chem) 2003;44:174–5.
[44] Aharoni SM. Macromolecules 1983;16:1722–8.
[45] Aharoni SM. Macromolecules 1986;19:426–34.
[46] Wool RP. Macromolecules 1993;26:1564–9.
[47] Based on published data, the entanglement molecular weight of PVA is assumed to 3750 g/mol.
[48] Komatsu M, Inoue T, Miyasaka K. J Polym Sci, Part B: Polym Phys 1986;24:303–11.
[49] For details of the experimental setup, the reader is referred to previous

publications from our group (e.g. Refs. [4,22] or Ref. [41] in this paper). Poly(vinyl alcohol) (PVA) (catalog # 36314-6; M_w=85–146k) was obtained from Aldrich Chemicals. For the electrospinning experiment, PVA solutions (6, 8 and 10 wt% in deionized water was prepared by heating the solution to 95 °C. In a typical experiment, a solution of polymer was drawn into a 5 ml syringe with a blunt needle at the end. The syringe with the needle was attached to the syringe pump (kdScientific, New Hope, PA). A high voltage supply (CZE 1000R) obtained from Spellman, NY was employed to obtain a field by connecting it to the blunt needle. The voltage was fixed at 25 kV and the source to target distance was kept at 20 cm for the PVA/water solutions. The flow rate was fixed at 4 ml/h. In order to obtain fibers for visualization by optical microscopy, the fibers were collected on glass slides covering a grounded metal target rotating at approximately 750–1000 rpm. Optical micrographs were obtained using an Olympus optical microscope (Olympus BE201).

[50] Sato T, Okaya T. Polym J (Tokyo, Japan) 1992;24:849–56.

[51] Lee KH, Kim HY, La YM, Lee DR, Sung NH. J Polym Sci, Part B: Polym Phys 2002;40:2259–68.

[52] Gupta P, Wilkes GL. Polymer 2003;44:6353–9.

[53] Doty P, Wagner H, Singer S. J Phys Colloid Chem 1947;51:32–57.

[54] Abied H, Brulet A, Guenet JM. Colloid Polym Sci 1990;268:403–13.

[55] There is some discrepancy in the published data for the entanglement molecular weight of PVC. The two most commonly reported values are 3125 g/mol (Refs. [44,45]) and 5500 gm/mol (Ref. [46]). For our calculations, we have employed the mean, i.e. 4310 g/mol.

[56] Poly(vinyl chloride) (PVC) (M_w=233k, catalog # 346764; M_w=106k, catalog # 346756) and solvents such as tetrahydrofuran, morpholine and dioxane were all obtained from Aldrich. In addition, higher M_w PVC (Geon 407; M_w unknown) was supplied to us by PolyOne. For the electrospinning experiment, PVC/THF, PVC/morpholine and PVC/dioxane solutions of different concentrations as described in the text were also prepared by heating the solutions to 70 °C. A voltage was adjusted to 15 kV and the tip to target distance of 20 cm was employed. The flow rate was fixed at 4 ml/h. In order to obtain fibers for visualization by optical microscopy, the fibers were collected on glass slides covering a grounded metal target rotating at approximately 750–1000 rpm. Optical micrographs were obtained using an Olympus optical microscope (Olympus BE201).

[57] Soenen H, Berghmans H. J Polym Sci, Part B: Polym Phys 1996;34:241–7.

[58] Hong PD, Chou CM, He CH. Polymer 2001;42:6105–12.

[59] Hong PD, Huang HT. Eur Polym J 1999;35:2155–64.